LABORATOIRE DE PHYSIQUE NUCLEAIRE

UNITE ASSOCIEE AU CNRS/IN2P3 (UA 57)

2, rue de la Houssinière 44072 NANTES CEDEX 03

NUCLEAR MATTER WITH PSEUDO-PARTICLE MODEL : STATIC BULK AND SURFACE PROPERTIES

D. Idier, B. Benhassine, M. Farine, B. Remaud, F. Sébille

Rapport Interne LPN - 93-03

UNIVERSITE DE NANTES

Nuclear matter with pseudo-particle model: static bulk and surface properties

D. Idier, B. Benhassine, M. Farine[1], B. Remaud, F. Sebille

Laboratoire de Physique Nucléaire CNRS/IN2P3, Université de Nantes

2, rue de la Houssinière 44072 Nantes, France

[1] Permanent address: Ecole Navale, Lanvéoc Poulmic, 29240 Brest Marine

ABSTRACT

Direct calculations of cold and hot nuclear matter (bulk and surface properties) are carried out within the frame of a pseudo -particle model using a gaussian decomposition of the distribution function. Comparisons with Hartree-Fock calculations, for a large class of effective interactions, show that such a model is reliable to reproduce accurately the equation of state of nuclear matter for large ranges of densities and temperatures. The number of gaussian per nucleon and the gaussian widths are critical parameters in that semi-classical model.

1. INTRODUCTION

Pseudo-particle models (PPM) have been extensively used to simulate heavy ion reactions at medium and high energies [1]. Although they were successful in describing many experimental features such as giant resonances excited during collisions, characteristics of the nuclear sidewards flow [2], as far as we know such models were never precisely tested against the Equation Of State (EOS) of nuclear matter. Obviously a good description of nuclear matter is required if we want to apply PPM to study clusterization in the spinodal region where initial conditions in (n,T) have to be precisely reproduced. In an other context, study of a very tenuous effect as isospin influence on heavy-ion collisions calls for an accurate description of the EOS [3]. This paper aimed at showing that such a program is possible using PPM.

Our calculations will be done in the framework of the so-called Landau-Vlasov model, which is the semi-classical version of the TDHF equation supplemented by the Uehling-Uhlenbeck collision term. Its special feature is the use of a continuous basis of gaussian packets (the pseudo-particles), with frozen width, to project the one-body phase-space Wigner function f(r,p) [4].

$$f(r,p;t) = \frac{1}{N}\sum_{k=1}^{NA} g_\chi(r-r_k)\,g_\phi(p-p_k) \qquad (1)$$

where the gaussian form factors in r and p space read respectively :

$$g_\chi(r) = \frac{1}{(2\pi\chi)^{3/2}}\exp\left(-\frac{r^2}{2\chi}\right) \quad ; \quad g_\phi(r) = \frac{1}{(2\pi\phi)^{3/2}}\exp\left(-\frac{r^2}{2\phi}\right) \qquad (2)$$

The sampling is done with a Monte-Carlo method [4]; N is the number of sampled gaussians per nucleon, A is the total number of nucleons and (r_k,p_k) are phase space centers randomly selected according to a density law which will be given farther. In general the phase-space has six dimensions and to cover each one uniformly with PP becomes rapidly hardly tractable. Some compromise has to be impose between the number of PP, their widths and the positions of their centers. Since Monte-

Carlo methods introduce statistical errors, the value of N will have to be larger than some critical N_c to insure numerical stability and reliable estimates of the observables. Influence of N and of the widths on bulk and surface properties of nuclear matter is carefully studied in sections 3 and 4 . Values for these parameters are given which insure stability for the observables.

2. EFFECTIVE INTERACTION AND FORMALISM

The PPM formalism will be used with nuclear effective interactions of the general form,

$$
\begin{aligned}
V(1,2) = &\sum_{c=1}^{n} t_c(r)\left[W_c + B_c P^\sigma - H_c P^\tau - M_c P^\sigma P^\tau\right] \\
&+ t_0(1+x_0 P^\sigma)\delta(r) \\
&+ t_1(1+x_1 P^\sigma)\frac{1}{2}\left[k'^2\delta(r) + h.c.\right] \\
&+ t_2(1+x_2 P^\sigma)k'\delta(r)k \\
&+ t_3(1+x_3 P^\sigma)n^\gamma(R)\delta(r)\ ; \qquad (3)
\end{aligned}
$$

with the usual notations :

$$
r = r_1 - r_2 \quad ; \quad R = \frac{r_1 + r_2}{2};
$$

$$
P_\sigma = \frac{1+\sigma_1\sigma_2}{2} \quad ; \quad P_\tau = \frac{1+\tau_1\tau_2}{2}.
$$

and is a gaussian form factor :

$$
f_c(r) = e^{-\left[r/\mu_c\right]^2}.
$$

The first term in V(1,2) is a finite range component and the remainder the usual Skyrme type interaction. P^σ and P^τ are respectively the exchange operators of spin and isospin coordinates and,

$$
k = \frac{\nabla_1 - \nabla_2}{2i} \quad ; \quad k' = -\frac{\nabla_1 - \nabla_2}{2i} \qquad (4)
$$

k is acting on the right and k' on the left.

A convenient representation of the two-body potential V(1,2) consistent with a semi-classical approach is provided by the Wigner transform in the phase space. The semi-classical Hartree-Fock potential then reads,

$$
\begin{aligned}
V_{HF}(r,p) = &\frac{3t_0}{4}n(r) + \left[\frac{3t_1 + (5+4x_2)t_2}{16}\right]\tau(r) \\
&+ \left[\frac{(5+4x_2)t_2 - 9t_1}{32}\right]\Delta n(r) + \frac{3t_3}{8}(\gamma+2)n(r)^{\gamma+1} \qquad (5) \\
&+ V_{HF}^{FR}(r,p)
\end{aligned}
$$

where the last term is the finite-range part of the interaction :

$$V_{HF}^{FR}(r,p) = \frac{1}{4}\sum_{c=1}^{n} s_c \int d^3r\, e^{-(r-r')^2/\mu_c^2} n(r)$$
$$- \frac{1}{4}\sum_{c=1}^{n} g_c \int d^3p\, e^{-(p-p')^2\mu_c^2} f(r,p) \qquad (6)$$

$$s_c = 4W_c + 2(B_c - H_c) - M_c$$
$$g_c = (W_c + 2(B_c - H_c) - 4M_c)\sqrt{\pi\mu_c^2}$$

f(r,p) is the one-body Wigner distribution function which is calculated from the one body density matrix n(r,r'),

$$f(r,p) = \frac{4}{h^3}\int ds \exp(-ip.s/\hbar) n\left(r + \frac{s}{2}, r - \frac{s}{2}\right) \qquad (7)$$

The local density n(r) is simply,

$$n(r) = \int dp\, f(r,p) \qquad (8)$$

and the kinetic energy density $\tau(r)$,

$$\tau(r) = \int dp\, \frac{p^2}{2m} f(r,p) \qquad (9)$$

Equations 5 and 6 provide the most general form of the nuclear effective interaction that we shall use, including both Skyrme and Gogny forces.

Substituting equation (1) in the expression for $V_{HF}(r,p)$ we get,

$$V(r,p) = \frac{3}{4}t_0 w\left(\sum_{i=1}^{NA} g_\chi(r - r_i)\right)$$
$$+ \frac{1}{32}\cdot[(5+4x_2)t_2 - 9t_1]\frac{w}{\chi^2}\left(\sum_{i=1}^{NA}\left[(r-r_i)^2 - 3\chi\right]g_\chi(r-r_i)\right)$$
$$+ \frac{3}{8}t_3(\gamma+2)w\left(\sum_{i=1}^{NA} g_\chi(r - r_i)\right)^{(\gamma+1)}$$
$$+ V^{FR}(r,p) \qquad (10)$$

$$V^{FR}(r,p) = w\sum_{c=1}^{n}\sum_{i=1}^{NA} s_c g_{\chi+\mu_c^2/2}(r - r_i)$$
$$+ w\sum_{c=1}^{n}\sum_{i=1}^{NA} g_c g_{\phi+2/\mu_c^2}(p - p_i) g_\chi(r - r_i) \qquad (11)$$

$w = 1/N$ is a constant weight insuring that f is normalised to the number A of nucleons. We have dropped the HF index to indicate that the above form applies only to pseudo-particle systems.The average potential acting on a PP is easily found by folding the potential V on the gaussian PP form factor. This procedure may induce some numerical difficulties [4] when powers of the local density are involved. In this case, we shall use the following approximation :

$$\left\langle n^{\sigma}(r)\right\rangle_{\eta} = \langle n(r)\rangle_{\eta}^{\sigma} = w^{\sigma}\left[\sum_{i=1}^{NA} g_{2\chi}(r_i - r)\right]^{\sigma} \qquad (12)$$

where $<>_{\eta}$ stands tor the folding operator on a gaussian centered at r_i.

This approximation is very good within the bulk of nuclear matter , but is certainly questionable in the surface part; this will be discussed in the next section on semi-infinite nuclear matter. Its effect is to rewrite the interaction as a function of <n> instead of n. The average potential is then obtained by simply changing χ in 2χ and ϕ in 2ϕ.

$$\langle V(r,p)\rangle_{\eta,p_i} = \frac{3}{4} t_0 w\left(\sum_{i=1}^{NA} g_{2\chi}(r - r_i)\right) + \ldots\ldots \qquad (13)$$

The one-particle energy for a PP centered at (r_i,p_i) is given by,

$$\varepsilon_i = \frac{p_i^2}{2m} + \langle V(r,p)\rangle_{\eta,p_i} \qquad (14)$$

in which we removed the self-energy of the PP. This prescription yields vanishingly small energies (as it should be) for the very dilute systems corresponding to sets of non-interacting pseudo-particles. The total energy can be expressed as,

$$E = \frac{1}{2} w\left[\sum_{i=1}^{NA} \langle V(r,p)\rangle_{r_i,p_i} - U^{res}(r)\right] + E_{kin} \qquad (15)$$

where,

$$U^{rea}(r) = \frac{3t_3}{8}\gamma w^{\gamma+1}\left[\sum_{i=1}^{NA} g_{2\chi}(r_i - r)\right]^{\gamma+1} \qquad (16)$$

is the rearrangement contribution to the one body potential coming from the density dependent part of the interaction. For E_{kin}, the kinetic contribution, we get,

$$E_c = w\sum_{i=1}^{NA}\frac{p_i^2}{2m} \qquad (17)$$

In the following all the calculations will be done for well known zero-range nuclear interactions, Tondeur functional To78 [5] , SkM* interaction [6] and the finite range force D1 of Gogny et al. [7].

3. INFINITE NUCLEAR MATTER

Infinite nuclear matter (INM) is an infinite system of nucleons characterised by a density n and a temperature T. It is a good approximation for bulk properties of large nuclei: we do have then to require that our model gives correct properties for INM: saturation energy curve, saturation density, incompressibility... . INM model was extensively used to calculate some parameters of mass formula [e.g. 8 and references included therein] difficult to extract from experimental values.

We simulate INM by imposing periodic boundary conditions to a cubic box of linear extension L. The sampling for f(r,p) is done as the following : the total number of PP (i.e. NA) is computed from two parameters, the number of PP per unit volume in momentum space and the spatial density. At first, momentum components are randomly sampled into a cubic area larger than Fermi sphere, say $2p_F$. Then, only PP whose momenta lay below a Fermi function,

$$f(p,T) = \frac{1}{1+\exp\left[-\frac{1}{2m^*T}(p^2-p_F^2)\right]} \qquad (18)$$

are kept. Fermi momentum p_F and effective mass m^*, at finite temperature come from Hartree-Fock calculations. Since we deal with uniform (infinite) systems the constant chemical potential is incorporated in the definition of p_F. The quantity N is, at last, simply computed as $N = N_S / nL^3$ where N_S is the final number of PP.

The linear extension of the box L has to be chosen in conjunction with the gaussians widths and the number of gaussians per nucleon N. The crucial importance of that choice was carefully studied, leading to take L larger than 9 fm to avoid discontinuities in the density due to periodic boundary conditions.

Figure 1 is of particular importance, showing that using less than 25 gaussians per nucleon will lead to a wrong energy, depending furthermore on the random number generator. The linear dimension of the box L is also a crucial choice as displayed on fig. 2. Influence of the position gaussian width is reported on fig. 3. Forthcoming calculations were all carried out using for those parameters values in their respective 'plateau region' to make them meaningful.

Figures 4, 5 and 6 show the energy per nucleon vs the density for the three considered interactions, for a large range of densities and three values of the temperature T=0, 5, and 10 MeV. These curves obtained from the simulation are checked against Hartree-Fock results. For the two zero-range interactions To 78 and SkM* the agreement for the hole range of densities and temperatures is striking. For Gogny D1 interaction this is not as good as for zero-range interactions; this can be understood reporting to (11). Comparing the partial contributions to the energy per nucleon obtained from the simulation and from Hartree-Fock calculations we evidenced that the discrepancy is coming from the exchange term. Representing the phase -space density by a sum of gaussians amounts to create a diffusivity in p which increase with (the parameter of eq. 2) ϕ : we checked that reducing ϕ will break uniformity of momentum space sampling and then worsen the results at densities above saturation. A way to cure that defect would be a slight redefinition of the finite range parameters, allowing a fit of the Hartree-Fock results at least around the saturation density.

A remarkable feature of our PPM model is its ability to describe quite well the whole EOS at different temperatures with values for the gaussian widths,

$$w_r = \sqrt{8\phi \mathrm{Log}2}$$
$$w_p = \hbar\sqrt{8\chi \mathrm{Log}2} \qquad (19)$$

which are independent of density and temperature, namely $w_r = 1.9$ fm^{-1} and $w_p/\hbar = .45$ fm^{-1}.

3. FROM SLAB TO SEMI-INFINITE NUCLEAR MATTER

The semi-infinite nuclear matter (SINM) model [9] consist of a medium which in two directions, called here x and y, is of infinite extent and constant density of nucleon ρ_0 ,

$$\rho(r) = \rho(z) \qquad (20)$$

but has a well defined surface perpendicular to the z-axis so that ρ(z) falls to zero for large values of z,

$$\rho(z) \to 0 \text{ as } z \to -\infty \qquad (21)$$

Note that ρ_0 has to be the saturation density of INM because the surface region of finite (and small) extent cannot modify the equilibrium properties of the limiting infinite region. SINM is expected to be a good representation for the surface region of large nuclei, allowing to study properties of that surface without being disturbed by curvature and higher order effects. [10, 11 and references quoted therein]

A simple way to simulate SINM from the model used in section II for INM is first to keep the periodic boundary conditions of INM for x,y directions and second to release the boundary condition in the z-direction. Instead of true SINM we then have a slab of thickness L. Increasing L (now independently of x and y dimensions) we should go closer to SINM and the slab density profile (more precisely the density profile of one half of the slab) will tend to the density profile of SINM.. At this stage, we have to point out that the value of L is crucial because of the desaturation phenomenon: if a nucleon system reaches a size comparable to the range of the nucleon-nucleon interaction, it loses its saturated structure [12].

Contrarily to INM where self-consistence is trivial, SINM has to find itself its equilibrium profile and Fermi energy. We simulated this feature as the following:

- The slab of thickness L is immersed in a larger one of thickness L' so that the system has room enough to look for its equilibrium configuration.
- The sampling is the same as for INM but is done for the larger slab

- We impose that the quantity,

$$B = \int_{-L/2}^{L/2} dz\, \rho(z) \qquad (22)$$

stays constant while the system is evolving towards equilibrium. We start the iterative procedure with an initial guess for the Fermi energy ε_F^0 and select the PP whose one particle energy (eq. 14) is lower than ε_F^0. We then calculate B using the PP inside the small slab. The next step is to vary ε_F^0 from $\pm$ $\Delta\varepsilon_F^0$ and to calculate the corresponding $B^{\pm}$ which will be used to estimate a correction to ε_F^0,

$$\varepsilon_F^0 = \varepsilon_F^0 + \Delta\varepsilon_F^0 \qquad (23)$$

The procedure is iterated until the Fermi energy stays constant. The surface energy coefficient a_S is calculated from the formula,

$$a_S = 4\pi r_0^2 \frac{E^{slab} - E^{INM}}{2L^2} \qquad (24)$$

where r_0 is the nucleon-nucleon average distance taken out of Hartree-Fock calculations for the given interaction. E^{slab} is the total energy computed in the slab of thickness L and E^{INM} the total energy for the same slab in INM.

Table 1 shows, for To 78, the sensitivity of a_S to the thickness L of the slab. We noted that desaturation is much more important than in ETF calculations of slab [12]; this is partly due to the width w_r of the gaussians which simulate an increase the range of nuclear forces; nevertheless the value of a_S is getting closer to Hartree-Fock value (20.0 MeV) as L increases.

Table 2 displays the good agreement between the values of a_S calculated with PPM and those from Hartree-Fock calculations for SINM [11] in the case of zero range interactions. Result for D1 case is not so good, as it was expected from problems we already met in infinite nuclear matter, but note that we have the right order of magnitude.

The numbers in brackets following the value of a_s are the differences between the largest and the smallest values (in MeV) computed over 100 initializations, varying the seed of the random generator : they differ from usual standard deviations which would be expected to be smaller.

Density profiles are reported on fig. 7 and 8 for To 78 and Skm*, showing the quality of PPM calculations. For Skm* the disagreement in the surface part is a consequence of all the approximations in the surface region (see our remark following equation (12)); it is not so significant for To 78 because for this interaction the effective mass is independent of the local density and then the only surface term, proportional to $\Delta\rho$, is calculated without approximations. The close-up on fig.9 displays the region where Hartree-Fock calculations give rise to Friedel oscillations; oscillations in the results of the simulation are, of course, of numerical origin as it is well-known that such a quantal effect is out of reach of semi-classical models [13] .

5. CONCLUSION

We have shown in this paper that PPM are reliable to represent bulk properties of cold and hot nuclear matter as well as surface properties of semi-infinite nuclear matter. Many precautions have to be taken concerning critical parameters as the number of gaussians per nucleon, size of the 'box' and width of the gaussians. The number of gaussians per nucleon has to be larger than 25 in order to avoid a too important dependence of the observables on the way the sampling is done.

Remarkably enough, we have shown that the EOS of nuclear matter (bulk and surface properties) can be reproduced with the same gaussian widths, namely w_r=1.9 fm and $w_p = .45\hbar$ fm^{-1} and this independently of the temperature T; this is moreover true for a large class of nuclear interactions, including finite range forces.

INM energies are precise enough (using large values for N) to give estimations of the incompressibility of INM, K_∞, in agreement with theoretical values for the zero-range interactions; for the Gogny D1 interaction the quality of the EOS around the saturation point prevents such an estimation.

PPM are then reliable to calculate parameters depending on the fine structure of the EOS. The latter statement is very important for the study of a phenomenon like clusterization which occurs in the spinodal region: the model should be able to discriminate between points inside and outside this region . Preliminary calculations are very encouraging and indicate that such a process could contribute to clusterization in heavy-ion reactions in the low energy regime. The preceding formalism is currently extended to include asymmetric hot INM and SINM and a semi-classical spin-orbit term.

REFERENCES

[1] G.F. Bertsch, S. Das Gupta, Phys. Rep. 160 (1988) 189

[2] Sebille, F., Royer, G., Grégoire, C., Remaud B., and Schuck, P. , Nucl. Phys. A501, 13(1989)

[3] Farine, M, Sami,T, Remaud, B.and Sebille, F, Z. Phys. A339 (1991) 363

[4] Grégoire, C., Remaud, B., Sebille, F., Vinet, L. and Raffray, Y., Nucl. Phys. A465, 77(1987)

[4] Schuck, P., et al., Prog. Part. Nucl. Phys. 22, L81 (1989)

[5] Tondeur, F., Nucl. Phys. A315, 353 (1978)

[6] Brack, M., Guet, C., Hakansson, H.B., Phys. Rep. 123 (1985) 276

[7] Dechargé, J. and Gogny, D., Phys. Rev. C 21 (1980) 1568

[8] Farine M., Pearson, J.M. and Rouben, B., Nucl. Phys. A304 (1978) 317

[9] Swiatecki, W.J., Proc. Phys. Soc. 64A (1951) 226

[10] Farine, M., Coté, J. and Pearson, J.M., Nucl. Phys. A338 (1980) 86

[11] Farine, M., Coté, J. and Pearson, J.M., Phys. Rev. C 24 (1981) 303

[12] Farine, M. and Stocker, W., Nucl. Phys. A459 (1986) 117

[13] Hohenberg, J.P. and Kohn, W., Phys. Rev. 136 (1964) 864

a hot

ve to

and

er to

rface

and

ss of

: the

s; for

a an

latter

the

: this

ould

alism

term.

Table 1:The dependence of a_S on the thickness L of the slab.

L (fm)	a_s (MeV)	Error bar (MeV)
13	34.5	(10.1)
16	28.1	(13.3)
18	25.7	(12.6)

Table 2 : The surface energy coefficient a_s calculated with the PPM for different interactions

Force	a_s (MeV) *(PP model)*	a_s (MeV) *(HF)*
To 78	25.8 (10.1)	20.0
Skm*	28.1 (17.0)	19.1
Gogny D1	42.8 (18.2)	21.0

Figure captions

Figure 1 : Saturation energy dependence on the number of gaussians per nucleon for To78 functional. Dashed line is obtained using NAG library random generator and solid line with Sobol sequences.

Figure 2 : Saturation energy dependence on the box size L for To78 functional

Figure 3 : Saturation energy dependence on the gaussian width for To78 functional

Figure 4 : Energy per nucleon in infinite nuclear matter for To78 functional

Figure 5: Energy per nucleon in infinite nuclear matter for Skm*

Figure 6 : Energy per nucleon in infinite nuclear matter for Gogny D1 interaction

Figure 7 : Density profile in semi-infinite nuclear matter for To 78 functional

Figure 8 : Density profile in semi-infinite nuclear matter for Skm*

Figure 9 : Fluctuations for the density, in the bulk part of semi-infinite nuclear matter, in the simulation and in Hartree-Fock calculations

18

o78

bol

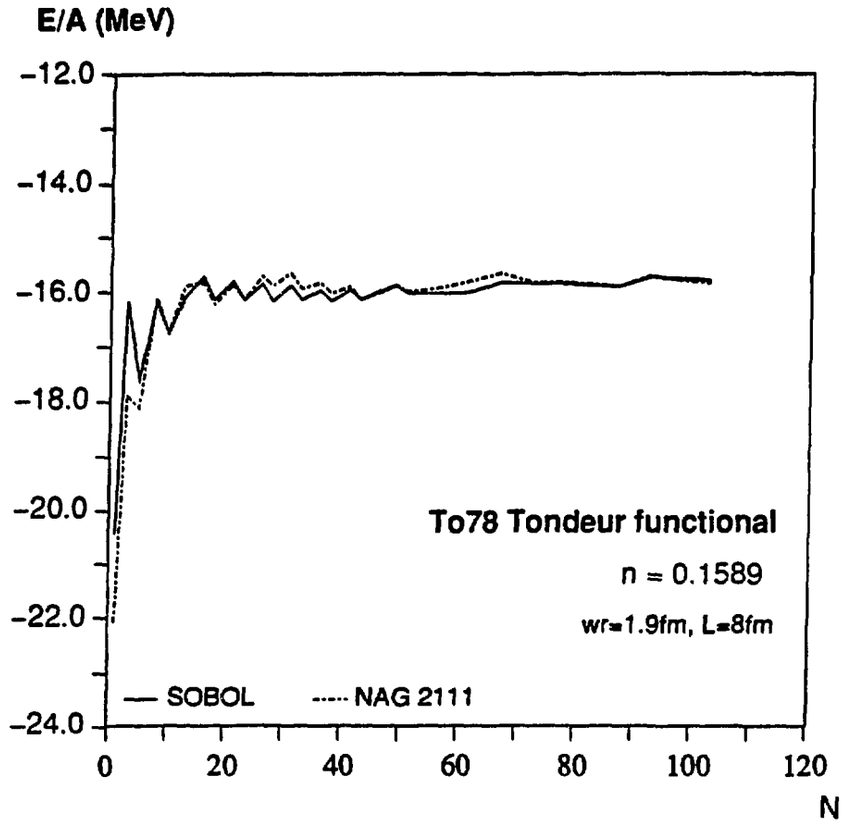

the

Figure 1

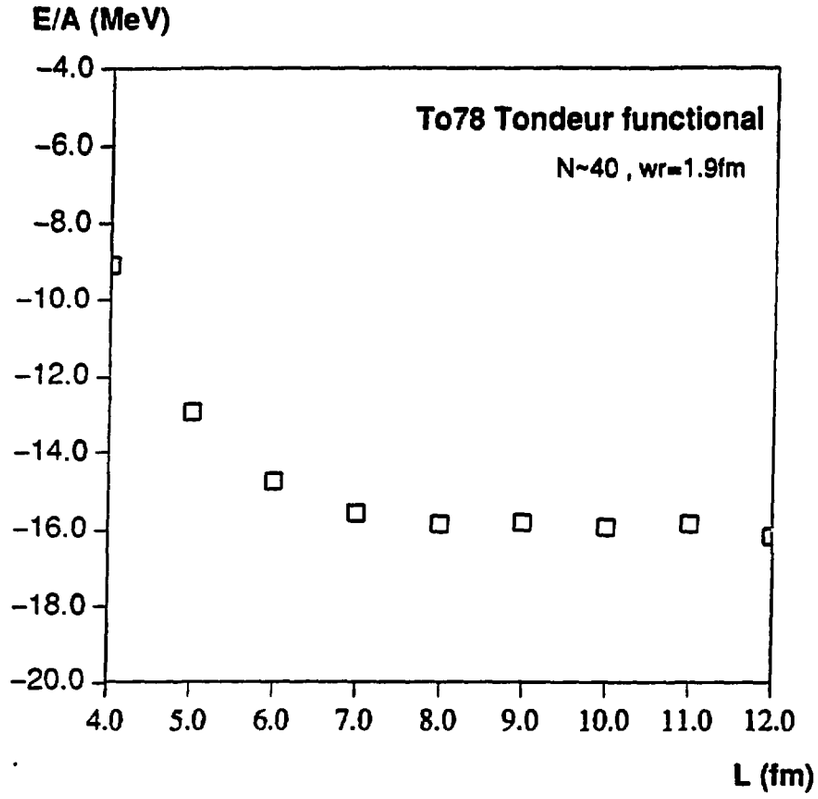
E/A (MeV)
-4.0
-6.0
-8.0
-10.0
-12.0
-14.0
-16.0
-18.0
-20.0
To78 Tondeur functional
N~40 , wr=1.9fm
4.0
5.0
6.0
7.0
8.0
9.0
10.0
11.0
12.0
L (fm)

Figure 2

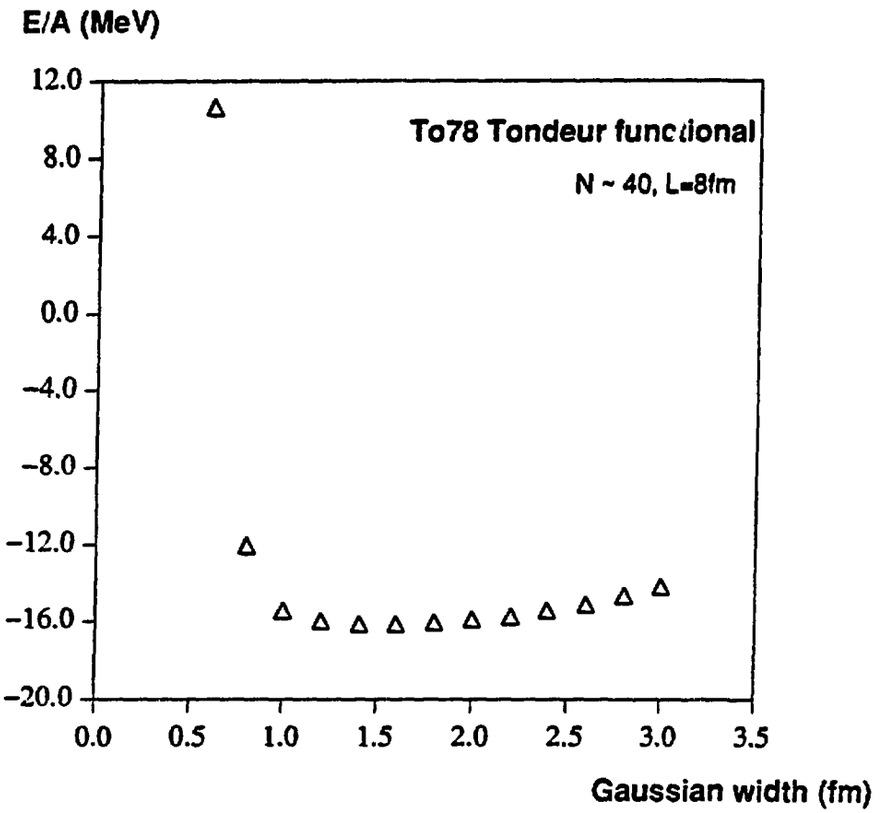
E/A (MeV)
12.0
8.0
4.0
0.0
−4.0
−8.0
−12.0
−16.0
−20.0
To78 Tondeur functional
N ~ 40, L=8fm
0.0
0.5
1.0
1.5
2.0
2.5
3.0
3.5
Gaussian width (fm)

Figure 3

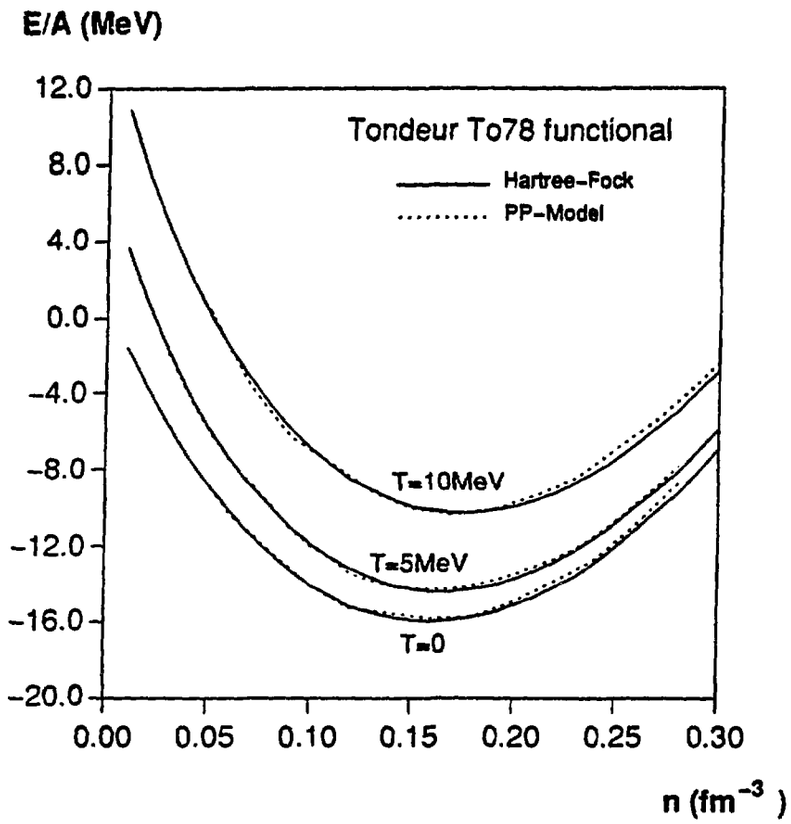
E/A (MeV)
12.0
8.0
4.0
0.0
-4.0
-8.0
-12.0
-16.0
-20.0
Tondeur To78 functional
Hartree-Fock
PP-Model
T=10MeV
T=5MeV
T=0
0.00
0.05
0.10
0.15
0.20
0.25
0.30
n (fm^{-3})

Figure 4

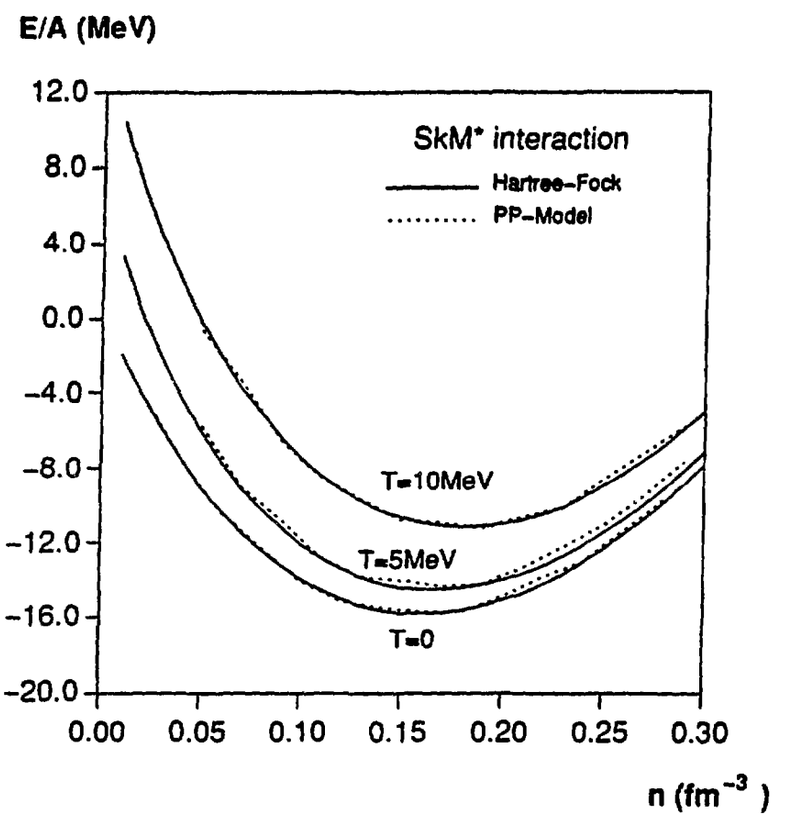
E/A (MeV)
12.0
8.0
4.0
0.0
-4.0
-8.0
-12.0
-16.0
-20.0
SkM* interaction
Hartree-Fock
PP-Model
T=10MeV
T=5MeV
T=0
0.00
0.05
0.10
0.15
0.20
0.25
0.30
n (fm^{-3})

Figure 5

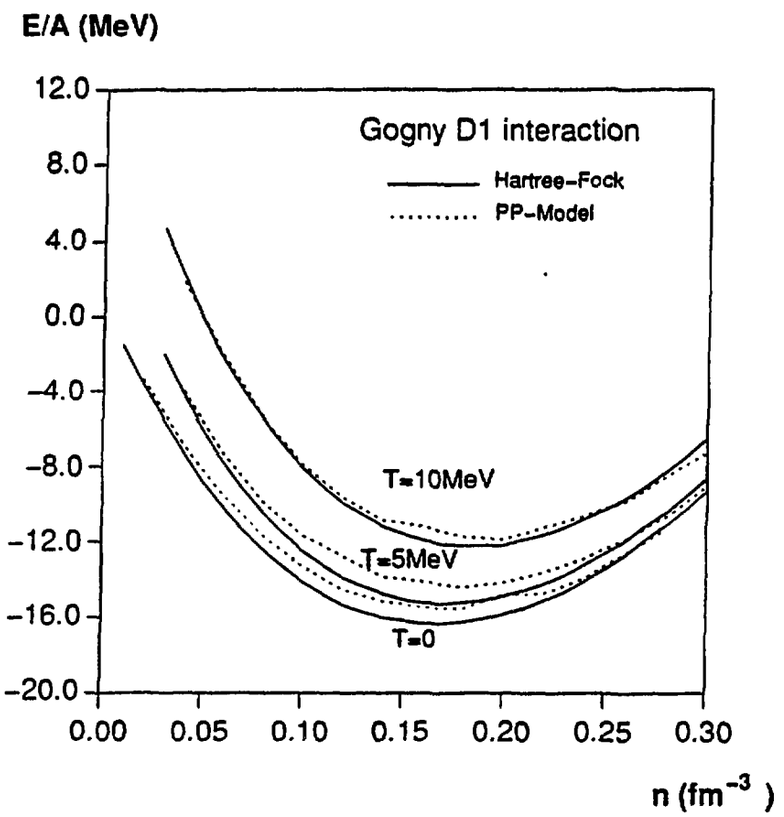
E/A (MeV)
12.0
8.0
4.0
0.0
−4.0
−8.0
−12.0
−16.0
−20.0
Gogny D1 interaction
Hartree-Fock
PP-Model
T=10MeV
T=5MeV
T=0
0.00
0.05
0.10
0.15
0.20
0.25
0.30
n (fm^{-3})

Figure 6

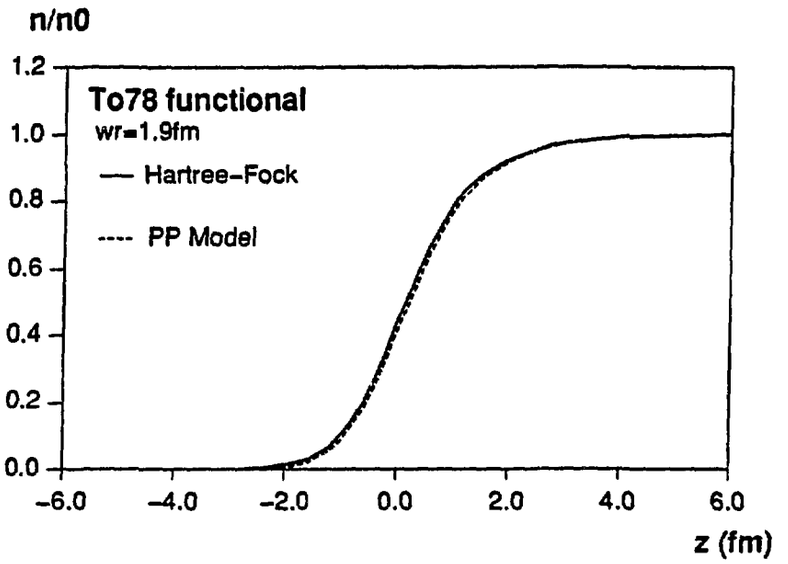
n/n0
1.2
1.0
0.8
0.6
0.4
0.2
0.0
To78 functional
wr=1.9fm
— Hartree–Fock
---- PP Model
–6.0
–4.0
–2.0
0.0
2.0
4.0
6.0
z (fm)

Figure 7

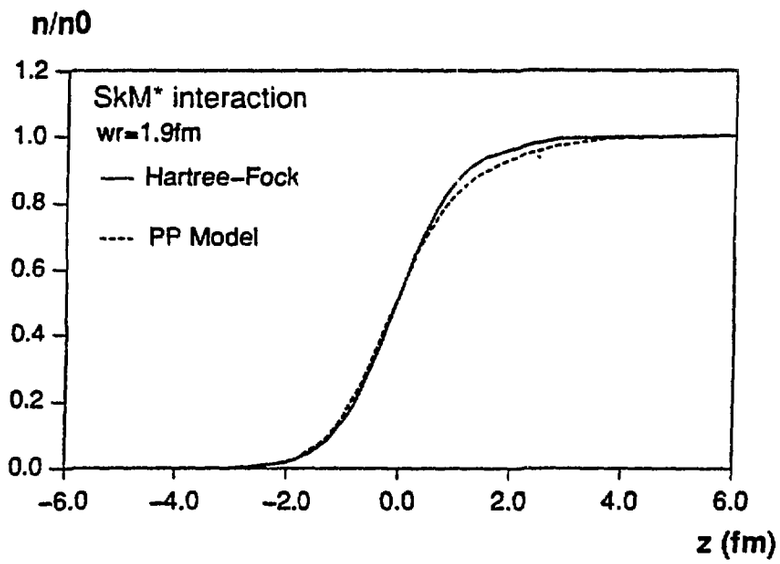
n/n0
1.2
1.0
0.8
0.6
0.4
0.2
0.0
SkM* interaction
wr=1.9fm
Hartree–Fock
PP Model
-6.0
-4.0
-2.0
0.0
2.0
4.0
6.0
z (fm)

Figure 8

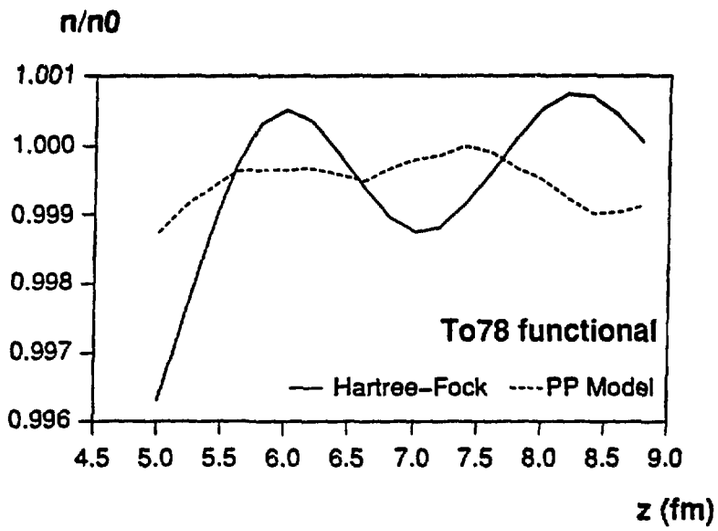
n/n0
1.001
1.000
0.999
0.998
0.997
0.996
4.5
5.0
5.5
6.0
6.5
7.0
7.5
8.0
8.5
9.0
z (fm)
To78 functional
Hartree-Fock
PP Model

Figure 9